Energy Management Control of Plug-in Hybrid Electric Vehicle using Hybrid Dynamical Systems

Harpreetsingh Banvait, *Student Member, IEEE,* Jianghai Hu, *Member, IEEE,* and Yaobin Chen, *Senior Member, IEEE*

***Abstract*—This paper presents a supervisory energy management control system design of power-split Plug-in Hybrid Electric Vehicles (PHEV). The power-split PHEV operates in various discrete operating modes. The dynamics of the system are continuous within each of these discrete modes. This power-split PHEV system consisting of discrete operational modes and continuous dynamics can be modelled using the hybrid dynamical system framework. In this paper, the vehicle and powertrain dynamics of power-split PHEV are introduced. Using these dynamics, a hybrid system model of the PHEV is proposed, and a nonlinear constrained energy minimization problem is solved using the dynamic programming approach. Furthermore, sub-optimal strategies for the energy minimization problem are obtained using model predictive hybrid control method. Simulation results show that, compared to the dynamic programming approach, the model predictive hybrid control provides good sub-optimal results and can be implemented in real-time.**

***Index Terms*—PHEV, MPC, Dynamic Programming, Hybrid system. Non-linear.**

NOMENCLATURE

J_e	Moment of inertia of engine and carrier gear.
J_r	Moment of inertia of ring gear.
J_g	Moment of inertia of generator and sun gear gear.
ω_e	Engine speed
ω_r	Ring gear speed
ω_g	Sun gear speed
τ_e	Engine torque
τ_g	Generator torque
τ_m	Motor torque
τ_s	Sun gear torque
τ_r	Ring gear torque
γ	Drivetrain from drive shaft to wheels
ρ	Planetary gear ratio
N_s	Number of teeth on sun gear
N_r	Number of teeth on ring gear
υ	Vehicle speed
R_w	Effective wheel radius
m	Mass of vehicle
F_{resis}	Resistive forces acting on vehicle
a_0, a_1, a_2	Resistive co-efficients
ρ	State of charge of battery
Q	Set of discrete states
X	Set of continuous states
V	Set of discrete inputs
Dom	Domain of mode
f	Continuous dynamics
E	Set of Events
G	Set of guard conditions
R	Set of resets
$Init$	Set of initial states
EV	Electric vehicle mode
$Regen$	Regenerative Braking mode
$Hybrid$	Hybrid vehicle mode
$Batterychg$	Battery charging mode
ω_e^{idle}	Engine idle speed
ω_e^{max}	Maximum engine speed
V_{oc}	Open circuit voltage of battery
P_{bat}	Power used from battery
R_{int}	Internal resistance of battery
C	Maximum capacity of battery
I	Battery Current
η_m	Motor efficiency
η_g	Generator efficiency
η_e	Engine efficiency
V_k	Value function at time k
σ	Mode

H. Banvait and Y. Chen is with is with the Department of Electrical and Computer Engineering, Purdue School of Engineering and Technology, IUPUI (e-mail: {hbanvait, ychen}@iupui.edu)

J. Hu is with the School of Electrical and Computer Engineering, Purdue University, West Lafayette, IN 47907 USA (email: jianghai@purdue.edu).

I. INTRODUCTION

IN today's world air pollution and dependence on fossil fuel have become huge problems. United States accounts for 22.6 % of the total oil consumption in the world and 42% of petroleum used in the US comes from foreign countries. In the US, 69% of the petroleum is used for transportation and the US transportation sector is heavily dependent on petroleum: 96% of total energy use in transportation comes from petroleum. Moreover, harmful gases like CO and CO_2 are emitted from transportation applications which accounts for 42% of air pollution in the US (96% of which comes from petroleum). Thus, reducing the petroleum usage for transportation purposes can reduce the depletion of fossil fuels, air pollution and reliance on external resources significantly.

One way to reduce the dependence on conventional sources of energy in transportation is by deploying Electric Vehicles (EVs) whose electrical energy is obtained from renewable energy sources. Due to technological limitations in battery technology, the development of EVs is confined. Hybrid electric vehicles, which use both internal combustion engine and battery as two different power sources, have been in the

market since late 1990s. Next step towards the transistion to EVs is Plug-in Hybrid Electric Vehicles (PHEVs), where the battery is the major power source as compared to the internal combustion engine.

In PHEVs both energy sources, a small onboard engine and a bigger battery pack, provide energy to drive the vehicle. The bigger battery pack cannot be charged from onboard internal combustion engine and must be charged from external power supply. Fig. 1 and Fig. 2 show the maximum torque curve and the efficiency countours of a typical engine and a motor, respectively. It can be seen from the figures that at high speeds the overall efficiency of the engine is low (at 20-22%) but it can produce large torque. The motor can produce very high torque at low speeds with very high efficiency around 85-90%; the Li-ion batteries and the motor combined have 80-90% efficiency. Battery and motor are highly efficient but motor can provide torque only at low speeds whereas engine can be efficient for high power demands. Using these two different energy sources together, an energy efficient vehicle can be designed. Hence, it has been of interest to researchers. In [1], Karbowski investigated a control strategy for pre-transmission parallel PHEVs using a global optimization technique based on the Bellman principle, with the main objective of increasing efficiency by reducing losses.

Additionally, the fuel economy of the vehicle can be improved by selecting optimal sizing of key vehicle driving components like motor, battery and engine. In [2], Baumann used a fuzzy logic controller for the nonlinear controller, presented system integration and component sizing techniques of the HEV, and simulated the system design and control strategy in an actual vehicle.

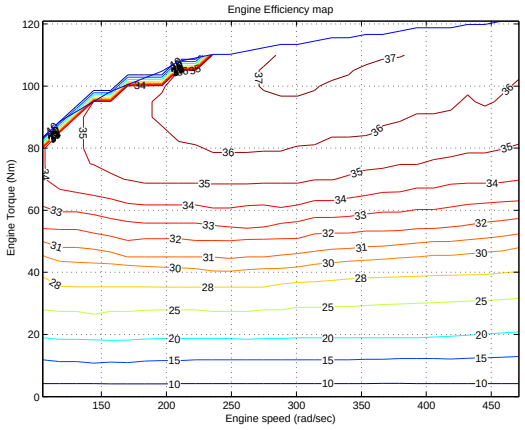

Fig. 1. Engine efficiency map contour.

Energy management system can be designed as rule-based strategies using heuristic knowledge. They are easy to implement and have been researched vastly. In [3], a rule based algorithm was used to solve the fuel minimization problem. [4] proposed a rule-based control strategy for a parallel PHEV bus model which showed better performance and higher engine efficiency. Sharer et al. compared EV and charge depletion strategy option using PSAT for different control strategies of power split HEVs [5]. Similarly, in [6] Gao et al. presented

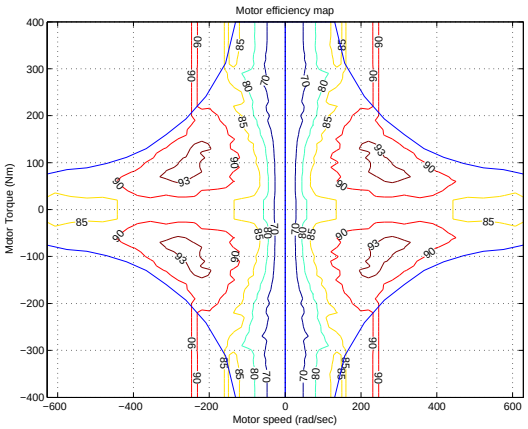

Fig. 2. Motor efficiency map contour.

various rule-based strategies for PHEV passenger cars and analyzed them in terms of fuel consumption. These rule-based energy management systems can be optimized by tuning its parameters. [7] did a parameteric optimization to optimize the control parameters using the Divided Rectangles (so-called DIRECT) method. They also analyzed the impact of distance travelled by PHEVs with these parameters. Similarly, Wu [8] employed a control parameter optimization for parallel PHEV using unconstrained PSO, with the target objective of the problem being the fuel economy along with the performance.

Design of energy management system of Power-split drivetrain PHEV requires a detailed Vehicle model. In [9] Cao et al. validated the PSAT model for the Toyota Prius PHEV which is a Power-split drivetrain; implemented control strategies to reduce the ON/OFF frequency of the engine by tuning some parameters, and also made the engine to operate in more efficient regions in the charge depletion (CD) state. Similarly, In [10], a detailed model of power-split HEVs was presented and the model was validated with test data. But in these vehicle models, discrete mode transitions were discarded and only continuous system models were considered.

Optimal Energy management system can be designed using dynamic programming. Several authors have used dynamic programming to design such system. [11] used a neural network to detect highway on/off ramps patterns through training from data sets. In [12] Moura et al. used a stochastic dynamic programming (DP) technique to obtain the optimal power management of a power split PHEV, implemented it for both blended fuel use strategy and charge depletion/charge sustaining modes, and studied the impact of battery size on these control strategies. His results showed that the blending strategy is significantly better for smaller batteries but its effect diminishes for large batteries. [13] used dynamic programming to get optimum energy distribution for certain drive cycles. Here the DP was implemented in the spatial domain while the drive cycle was approximated which showed that the time for the DP calculations can be reduced to get suboptimal results. Gong et al. Liu [14] obtained the vehicle dynamics for power-split HEV and designed energy management using stochastic dynamic programming and ECMS strategy and compared

the results with those using dynamic programming. Additionally, Energy management system can be designed using other optimal theories. In [15] Stockar designed a supervisory energy manager by applying Pontryagin's minimum principle to minimize the overall carbon dioxide emissions. Borhan [16] employed model predictive control strategy to design a power management system of power-split HEVs. Musardo [17] designed a real-time Adaptive Equivalent Consumption Minimization Strategy (A-ECMS) for energy management system of HEV, whereas in [18] a Particle Swarm Optimization (PSO) based solution is proposed.

The optimal energy management system cannot always be applied in real-time. Hence, several authors have proposed sub-optimal energy mangement systems. Xiao [19] also used PSO to obtain optimal solutions and subsequently used Artifical Neural Network (ANNs) to produce sub-optimal results. In [20] Mohebbi et al. showed that a neural network based adaptive control method can be used for controlling PHEVs. This leads to an online controller that can maximize the output torque of the engine while minimizing the fuel consumption. [21] used artificial neural networks and fuzzy logic to implement a load leveling strategy for intelligent control of a parallel HEV powertrain. [22] developed and tested a highly efficient energy management system for HEVs with ultracapacitors using neural networks. They first obtained an optimal control model and then obtained its numerical solution. Gong [23] used dynamic programming along with intelligent transport system GPS, Geographical Information System (GIS) and advanced traffic flow modeling technique to obtain an optimized power management strategy for a parallel PHEV. Moreno et al.

In PHEVs, the vehicle operates in various modes such as the EV mode, the Battery charging mode, the Regenerative mode, etc. In each of these modes, the vehicle dynamics is different. Furthermore, the inputs of engine and motor in these modes are also different. Such a system which consists of both discrete and continuous states can be modelled by hybrid dynamical systems. Yuan [24] demonstrated the application of hybrid dynamical systems to HEVs, where sequential quadratic programming and dynamic programming were used to obtain an optimal solution to the problem before using fuzzy approximation to obtain sub-optimal ones.

The contributions of this paper consists of the following: i) a model of the power-split PHEV using hybrid dynamical system; ii) the design of an energy management strategy based on the dynamic programming approach of hybrid systems; iii) a sub-optimal strategy using model predictive hybrid control. This paper is organized as follows. Section II presents vehicle model of the power-split PHEVs. It the provides detailed dynamics of the power-split drivetrain; and using these dynamics vehicle dynamics, a hybrid dynamical system framework model of the power-split PHEV is presented. Section III formulates the energy minimization problem of PHEV, and presents the detailed design of the supervisory energy management strategy. The dynamic programming and model predictive hybrid control based solutions are also presented. Finally, Section IV presents the simulation results of the proposed strategies and compares their performances.

II. Nonlinear PHEV Model

The drivetrain of conventional vehicles consists of gearbox, clutch and engine; and there is only one path for energy to flow and one degree of freedom. In comparison, power-split drivetrain has two paths of energy flow, i.e. electrical path and mechanical path. Hence, power-split drive train has two degrees of freedom: engine speed and engine torque. The power-split drivetrain has a continuously varying transmission consisting of planetary gear set. Fig. 3 shows a detailed structure of the power-split drivetrain. The PHEV consists of a speed coupling between the engine and the generator (MG2); and a torque coupling between the planetary gear output and the motor (MG1). The engine is connected to the carrier gear of the planetary gear set and the generator is connected to the sun gear of the planetary gear set. The output of this planetary gear set, ring gear, is connected to the motor (MG1) via torque coupling. The output of this torque coupling is connected to the drive shaft, the final drive, the axle and the wheels, respectively. Fig. 4 shows the energy flow in PHEV power-split drivetrain. The power delivered by the engine is split into the electrical path and the mechanical path. Part of the power delivered by engine P_E is converted into electrical power P_{EG} due to the reaction torque provided by the generator. The

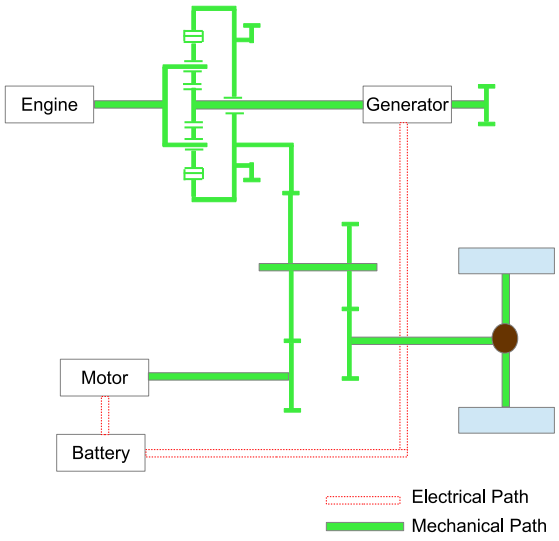

Fig. 3. Power split Drive train configuration.

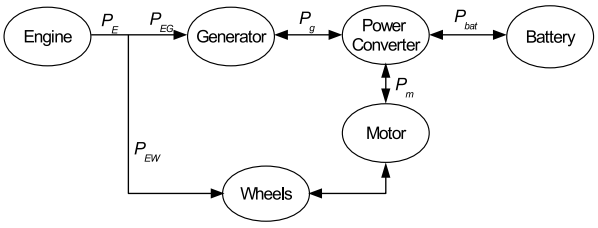

Fig. 4. Energy flow in Power split drivetrain.

remaining power P_{EW} is delivered mechanically directly to the wheels using the ring gear of the planetary gear set. The electrical power from the generator P_g is provided to the power converter which routes it to the motor P_m and the rest of the electrical power P_{bat} is deposited into the battery.

A. PHEV Vehicle Dynamics

By applying the Newtons second law on the engine we obtain the equation (1) below which relates the engine speed ω_e with the engine torque τ_e, the sun gear torque τ_s and the ring gear torque τ_r:

$$J_e\omega_e = \tau_e - \tau_r - \tau_s. \tag{1}$$

Similarly, applying the Newtons law at the ring gear we obtain the equation (2) which relates the ring gear speed ω_r with the ring gear torque τ_r, the motor torque τ_m and wheel torque τ_w:

$$J_m\omega_r = \tau_r + \tau_m - \gamma\tau_w. \tag{2}$$

The generator speed ω_g is related to the generator torque τ_g and the sun gear torque as

$$J_g\omega_g = \tau_g + \tau_s. \tag{3}$$

In equations (1), (2) and (3), J_e, J_m, J_g are the moment of inertia of the engine, the motor, and the generator, respectively, and γ is the gear ratio.

Due to the kinematic property of the planetary gear set, the sun gear, the carrier gear and ring gear are linearly related to each other. Since the sun gear is connected to the generator (MG2), the carrier gear is connected to the engine and the ring gear is connected to the output shaft, the engine speed ω_e, the generator speed ω_g and the ring gear speed ω_r are related by:

$$\omega_r = (1+\varrho)\omega_e - \varrho\omega_g. \tag{4}$$

In the above speed coupling relation, ϱ is the planetary gear ratio defined by

$$\varrho = Ns/Nr, \tag{5}$$

where N_s and N_r are the numbers of gear teeth on the sun gear and the ring gear, respectively. Note that since the moment of inertia of the pinions gears is very small, they are neglected when compared with the moments of inertia of the engine, the motor, and the ring gears.

The sun gear torque τ_s and the ring gear torque τ_r are related by:

$$\tau_s = \varrho\tau_r. \tag{6}$$

For this drivetrain, the motor is on the driveshaft connected by the ring gear. Thus, the ring gear speed ω_r is the same as the motor (MG1) speed ω_m. The relation between the motor speed ω_m and the vehicle speed υ is given by

$$\omega_m = \frac{\upsilon}{R_w\gamma}. \tag{7}$$

By applying the Newton's second law to the vehicle dynamics, the following equation is obtained which relates the vehicle speed υ, the wheel torque τ_w and the losses F_{res} as:

$$R_w m\dot{\upsilon} = \tau_w - mF_{res}. \tag{8}$$

In this equation, R_w and m are the wheel radius and the vehicle mass, respectively.

The vehicle has to overcome resistance from aerodynamic forces and rolling resistance losses. To account for this, a resistive force F_{res} is introduced, which can be approximated as a quadratic function of the vehicle speed υ as:

$$F_{res} = a_0 + a_1\upsilon + a_2\upsilon^2. \tag{9}$$

Here, the parameters a_0, a_1 and a_2 have been obtained from experimental results of the PSAT software.

The PHEV battery is modelled as an equivalent open circuit model. The current drawn from the battery is given by

$$I = \frac{V_{oc} - \sqrt{V_{oc}^2 - 4R_{int}P_{bat}}}{2R_{int}}. \tag{10}$$

A negative current I implies that the current goes into the battery. In this equation, C is the maximum capacity of the battery, R_{int} is its internal resistance, V_{oc} is the open circuit voltage of the battery and P_{bat} is the battery power.

Power P_{bat} drawn from the battery is further given by

$$P_{bat} = \frac{\omega_m\tau_m}{\eta_m(\omega_m,\tau_m)} + \omega_g\tau_g\eta_g(\omega_g,\tau_g). \tag{11}$$

Here, η_m is the motor efficiency as a function of the motor torque τ_m and the motor speed ω_m. Similarly, the generator efficiency η_g depends on the generator torque τ_g and the generator speed ω_g.

Using the battery current I in (10), differential equation of the State of Charge (SOC) ρ of the battery is obtained as:

$$\frac{d\rho}{dt} = \frac{1}{2R_{int}C}\{-V_{oc} + \sqrt{{V_{oc}}^2 - 4R_{int}P_{bat}}\}. \tag{12}$$

The engine power is split into the mechanical power and the electrical power by the generator speed. The generator speed is changed using the reaction torque provided to the engine through the generator torque. This generator torque is then transmitted to the wheels via the planetary gear set. The generator (MG2) acts as the motor when both the speed and the torque are acting in the same direction; otherwise it acts as a generator. When the generator (MG2) is acting as a generator, absorbing mechanical power of the engine and converting it into electrical power, the drivetrain is operated as a positive split mode, which occurs when the battery (or the driver) demands more power from the vehicle. Generator (MG2) can also act as a motor by providing reaction torque to the engine and delivering power to the wheels using the planetary gear set. This mode of operation is called the negative split mode, which occurs when the demanded power is suddenly reduced.

B. Hybrid System Model of PHEV

Power-split Plug-in Hybrid Electric Vehicle (PHEV) operates in different modes. When the power demand is low and the vehicle speed is low, PHEV can be operated in the EV mode because it is more efficient for the energy to flow from the battery to the motor. Fig. II-B shows the energy flow in the EV mode. When the vehicle is decelerating rapidly, the kinetic energy of the vehicle can be recovered by operating the motor (MG1) as a generator to recover maximum electrical energy

from the vehicle deceleration. This operation of the vehicle is called the regenerative braking mode. The energy flow during the regenerative braking mode is shown in Fig. II-B. It can be seen that the motor (MG1) recovers the energy and stores it back into battery. When the power demand is high so that the motor (MG1) alone cannot supply it, the vehicle can be operated in the hybrid drive mode. Fig. II-B shows that during this mode the motor (MG1) gets power from the battery to drive the wheel and at the same time the generator (MG2) is also acting as a motor and provides the reaction torque to the engine and powers the wheels usingthe planetary gear set. When the battery power is not sufficient, the battery can be charged using the onboard engine. To do this, the generator (MG2) stores energy into the battery. At the same time, the motor (MG1) can provide power to the wheels if the battery has sufficient power. Fig. II-B shows the energy flow during the battery charge mode. Since the operation of the PHEV is different in each mode, it can be modelled by a hybrid dynamical system. A hybrid dynamical system model of the PHEV is given by $H_s = (Q, X, V, Dom, f, E, G, R, Init)$.

1) Continuous states set $X = \{\omega_e, \upsilon, \rho\}$: engine speed ω_e, vehicle speed υ and State of Charge(SOC) ρ of the battery;
2) Continuous input $V = \{\tau_e, \tau_g, \tau_m\}$: engine torque τ_e, generator (MG2) torque τ_g and motor (MG1) torque τ_m;
3) Set of discrete states $Q = \{Regen, EV, Hybrid, Batterychg, ED\}$;
4) Domain $Dom(\cdot) : Q \to \mathbb{R}^n$ specifies the set of feasible continuous state for each mode:

$$Dom(EV) = \{x : \omega_e = 0, \upsilon > 0, 0.3 < \rho < 1\}$$

$$Dom(Regen) = \{x : \omega_e = 0, \upsilon > 0, 0 < \rho < 0.9\}$$

$$Dom(Hybrid) = \{x : \omega_e^{idle} \leqslant \omega_e \leqslant \omega_e^{max}, 0 < \upsilon, 0.25 < \rho < 0.3\}$$

$$Dom(Batterychg) = \{x : \omega_e^{idle} \leqslant \omega_e \leqslant \omega_e^{max}, 0 < \upsilon, 0.25 < \rho < 0.3\}$$

Thus, in EV mode and Regen mode, ω_e is zero. For the remaining modes ω_e is within its lower bounds of ω_e^{idle} and its maximum ω_e^{max}. In EV mode, ρ is not allowed to discharge more then 0.25, otherwise it will reduce the battery life. In Regen mode, ρ is restricted to 0.9 so that the battery always has capacity to collect energy. In Hybrid and Batterychg modes, ρ is required to be between 0.25 and 0.3 to maintain the SOC.

5) Continuous dynamics $f = Q \times X \times V \to \Re^n$ defines the dynamics of the continuous states X in each mode Q, which has been derived in (1-12). In particular, the dynamics in EV mode and Hybrid drive mode are given in (15) and (16), respectively, with α and $Jr_d^{'}$ given by

$$\alpha = J_g J_r'(\varrho + 1)^2 + J_e J_r' \varrho^2 + J_e J_g, \quad (13)$$

$$J_r' = J_r + m(R_w \gamma)^2. \quad (14)$$

For Regen mode the dynamics is the same as that of the EV mode, and the dynamics of the Batterychg mode is the same as that of the Hybrid mode but with different inputs and state constraints as defined by their respective domains;

6) Set $E \subset Q \times Q$ of transistions between modes;
7) Set $G(\cdot) : E \to 2^X$ of guards defined for each $e = (q, q') \in E$;
8) Set $R(\cdot) : E \times X \to 2^X$ of reset maps. For this system, the engine speed ω_e is reset to zero whenever the system enters EV mode or Regen mode;
9) Set $Init \subset Q \times X$ of initial states.

III. Hybrid Control Architecture

The driver of a vehicle provides its input using an accelerator and a brake pedal. Based on this driver input, a supervisory vehicle controller calculates the torque demanded by the driver. Fig. 6 shows the hierarchy of energy management control for a power-split PHEV. As shown, an optimal control mode is selected according to the driver torque dmand, which provides the optimal motor torque Tm, engine torque Te and generator torque Tg. These torque demands are then sent to the low level motor controller, engine controlle and generator controller, respectively. Using these command torques, the engine controller determines the amount of fuel to be injected; and controllers of the motor and the generator determine the amount of current to be provided. Based on these actuating signals sent by the low level controllers, the PHEV engine, motor and generator produce the demanded torque to drive the vehicle. Finally, various sensors on the vehicle send the feedback signals back to the supervisory vehicle controller for its decision making.

The operational modes of PHEVs are shown in Fig. 7. In a PHEV, it is desired to maximize the use of electrical energy because it is cost effective and abundantly available. Thus, starting from 95% SOC, the vehicle operates in the EV mode and the Regen mode according to Fig. 7. As soon as the SOC reaches 30%, the depletion of SOC of battery should be controlled because excess of discharge of battery would reduce the battery life. Hence, to reduce the further rapid depletion of SOC, it can be operated in the Hybrid mode, Batterychg mode EV mode or Regen mode. Vehicle can operate in one of these modes such that objective is minimized, vehicle performance is as desired, and the SOC of the battery will not fall below its minimum value. Due to these multiple solutions trajectories, when the SOC is between 25% and 30%, an energy minimization optimization problem can be formulated such that optimum mode and optimum trajectory can be evaluated.

A. Dynamic Programming

Dynamic programming is an optimization method for obtaining a global optimum solution to the optimal control problems. This optimization method can be used to solve complex problems, such as nonlinear constrained optimization problems which have constraints on both the states and the inputs. The main drawbacks of the dynamic programming method are that the disturbances have to be assumed known in advance over the period of time and that it is computationally very

$$\begin{aligned}\dot{\omega_e} &= 0\\ \dot{\nu} &= \frac{\tau_m}{J_r + J_g/\varrho^2} - \frac{\tau_g}{\varrho(J_r + J_g/\varrho^2)} - \frac{\gamma R_w F_{resis}}{J_r + J_g/\varrho^2}\\ \dot{\rho} &= \frac{1}{2R_{int}C}\{-V_{oc} + \sqrt{{V_{oc}}^2 - 4R_{int}P_{bat}}\}\end{aligned} \tag{15}$$

$$\begin{aligned}\dot{\omega_e} &= \frac{1}{\alpha}\{(\varrho^2 J_r' + J_g)\tau_e + (1+\varrho)\varrho J_r'\tau_g + J_g\tau_m - (1+\varrho)J_g r\gamma F_{resis}\},\\ \dot{\nu} &= \frac{1}{\alpha}\{(1+\varrho)J_g\tau_e + (-\varrho J_e)\tau_g + ((1+\varrho)^2 J_g + \varrho^2 J_e)\tau_m - ((1+\varrho)^2 J_g + \varrho^2 J_e)R_w\gamma F_{resis}\}.\\ \dot{\rho} &= \frac{1}{2R_{int}C}\{-V_{oc} + \sqrt{{V_{oc}}^2 - 4R_{int}P_{bat}}\}\end{aligned} \tag{16}$$

expensive. Due to these drawbacks, dynamic programming cannot be applied in real-time in most of the cases. But such a drawback can be alleviated by knowing the stochastic properties of the disturbances in advance and using them in the dynamic programming procedure. Such an approach is called stochastic dynamic programming, and can act as a benchmark for other sub-optimal real-time approaches.

Dynamic programming can be divided into two phases. In the first phase, all the value functions are evaluated backward in time at every time interval, at every state and at every mode as shown in Fig. 8. Once all the value functions have been evaluated, in the second phase, an optimal control sequence is recovered using forward time evaluations. The results obtained by the exact dynamic programming method are in general globally optimal. However, to reduce complexity, the method to be presented in this section employs state space discretization and objective function approximations. As a result, the obtained results are sub-optimal.

The dynamic programming method can be briefly described as follows. In all steps only the feasible states are considered whereas the infeasible states are discarded by assigning infinite cost to them. Starting at the final time N, the value function of all the states are initialized as zero. Then at time step $k = N-1, \ldots, 0$, the value function $V_k(x_k)$ for a feasible current state x_k is the minimum of the sum of the current time step cost $w(x_k, u_k, \sigma_{k+1})$ and the cost-to-go from the next state $V_{k+1}(x_{k+1})$, with the minimum taken over all the continuous controls u_k and modes σ_{k+1}. Here, the current cost $w(x_k, u_k, \sigma_{k+1})$ is a function of the current feasible state x_k, the current feasible inputs $u_k(k)$, and the mode σ_{k+1}. The cost-to-go from the next state $V_{k+1}(x_{k+1})$ is a function of the next state x_{k+1} under the inputs u_k and σ_{k+1}. More precisely,

$$\begin{aligned}V_k(x_k) = \min_{u_k, \sigma_{k+1}} [&w(x_k, u_k, \sigma_{k+1}) +\\ &V_{k+1}(x_{k+1}(x_k, u_k, \sigma_{k+1}))].\end{aligned} \tag{17}$$

This iteration is continued until the value function $V_0(\cdot)$ is computed. After evaluating the value functions at each state and time, the optimal input u_k^* and optimal mode σ_{k+1}^* can be recovered at each time step k using (17), by going forward in time starting from the given initial state x_0.

High computational complexity is a major drawback of the dynamic programming method. The computational time increases linearly with the time horizon N but exponentially with the state dimension n and the control input dimension m. An upper bound on the computational time of the dynamic porgramming method is shown in (18) as

$$O(N \cdot p^n \cdot q^m), \tag{18}$$

where p and q are the numbers of possible states and inputs, respectively. The PHEV optimization problem solved in this paper is of lower order but has a long time horizon.

1) Problem Formulation: As shown in Fig. 7, when the SOC of the battery is more than 30%, the vehicle operates in either the EV mode or the Regen mode depending on the power demand by the driver. But when the SOC is less then 30% then the vehicle can be operated either in EV mode, Regen mode, battery charge mode or hybrid drive mode. The selection of one of these modes can be formulated as an optimal control problem. An energy minimization problem can be defined as:

$$\begin{aligned}\underset{u(t)\in U, \sigma(t),\ t\in[t_0,t_f]}{\text{minimize}} \quad & J(x(t), u(t))\\ \text{subject to} \quad & \dot{x} = f(x,u)\\ & x \in X\\ & u \in \Omega,\end{aligned} \tag{19}$$

where X is the domain of each mode, and U is the input constraint set defined by:

$$\begin{aligned}\tau_e^{min} < \tau_e < \tau_e^{max}\\ \tau_g^{min} < \tau_g < \tau_g^{max}\\ \tau_m^{min} < \tau_m < \tau_m^{max}.\end{aligned} \tag{20}$$

The performance of the PHEV can be evaluated in terms of its energy usage, fuel consumption, emissions, etc. In PHEV, the fuel consumption is reduced significantly due to the electrical energy usage, and can be further improved by optimizing the use of fuel and electrical energy. To accomplish this objective, an objective function of the total energy use by the PHEV is defined below:

$$J(x(t), u(t)) = \int_{t_0}^{t_f} \frac{\omega_e \tau_e}{\eta(\omega_e, \tau_e)}\, dt + \zeta(\rho(t_f) - \zeta\rho(t_0)). \tag{21}$$

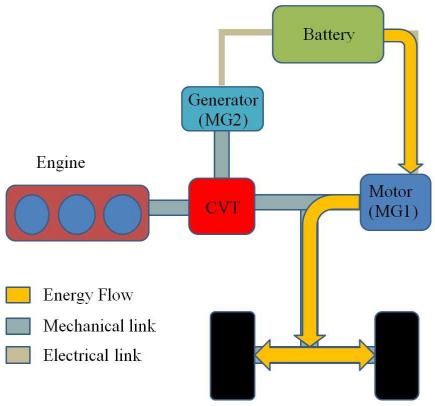

(a) EV mode

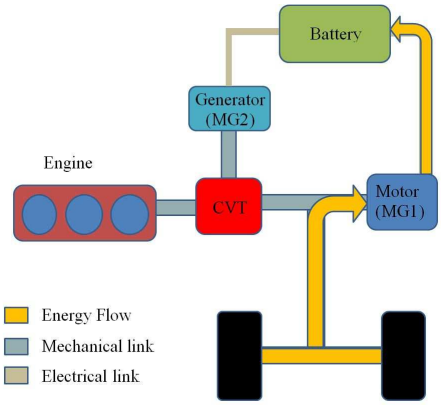

(b) Regenerative Braking mode

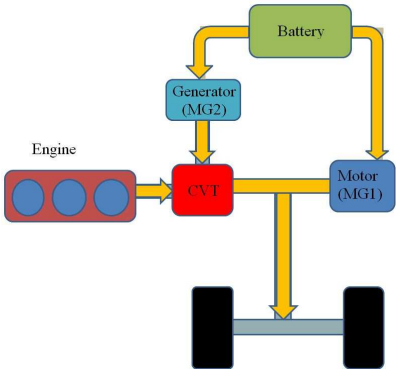

(c) Hybrid drive mode

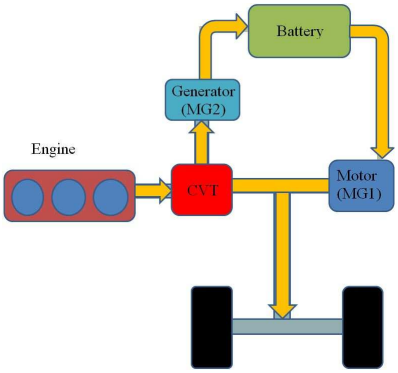

(d) Battery charge mode

Fig. 5. Hybrid Vehicle operating modes

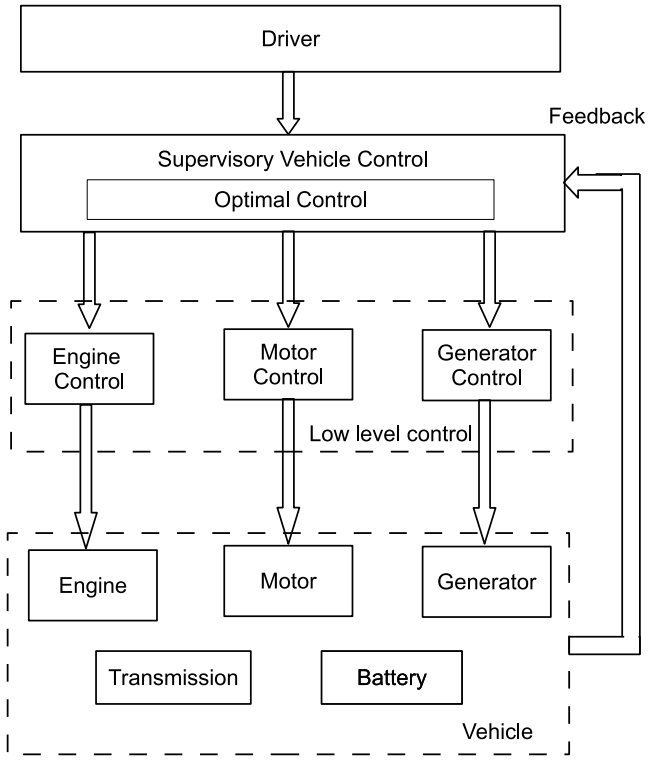

Fig. 6. Hierarchy of control in Power split Drive train.

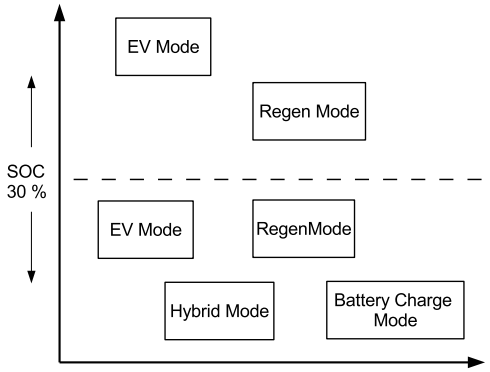

Fig. 7. Power split drive train operational modes

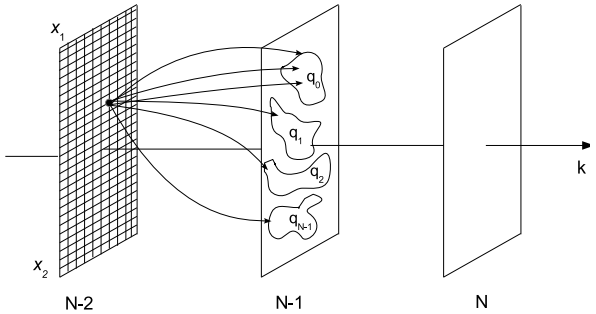

Fig. 8. Dynamic programming value iteration.

In (21), the integration term is the energy usage by the engine, the second term is the equivalent energy usage by the battery during the time period $[t_0, t_f]$. Here, $\rho(t_0)$ and $\rho(t_f)$ denote the energy stored in the battery at the initial and the final times, respectively, and $\zeta(\cdot)$ is a mapping that characterizes the equivalent energy usage corresponding to a certain battery drainage.

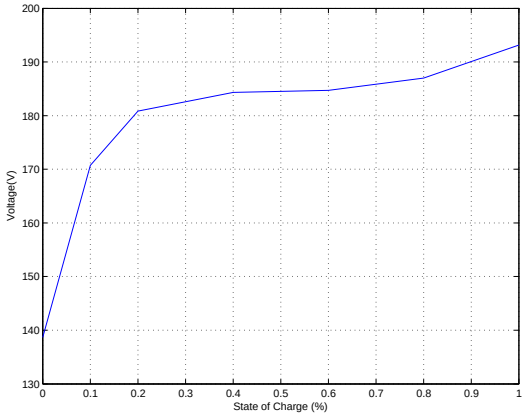

Fig. 9. Open circuit voltage of battery.

B. MPC Hybrid Control

An alternative control method is by the model predictive control (MPC). In model predictive control, the optimal control sequence u and the optimal mode sequence σ are obtained progressively based on the prediction of a future moving time horizon. When the time horizon is short, MPC can be computed much more efficiently than the dynamic programming method, even in real time.

Fig. (10) shows the implementation of the model predictive control on the hybrid system model of the PHEV. At each particular sampling time k, the optimal control sequence $u(k|k), u(k+1|k) \cdots u(k+N-1|k)$ and the optimal mode sequence $\sigma(k+1|k), \sigma(k+2|k) \cdots \sigma(k+N|k)$ is computed over the prediction time horizon $k, k+1, \ldots, k+N$. While obtaining the optimal control, it is assumed that prior knowledge of the disturbances to the system is known. The predicted state trajectory at the sampling time k is evaluated by

$$x(k+1+i|k) = A(i)x(k+i|K) + B(i)u(k+i|k) \quad \forall i = 0, 1, \ldots, N-1. \tag{22}$$

Here, $x(k+1|k)$ and $u(k+1|k)$ denote the state $x(k+1)$ and the input $u(k+1)$ at time $k+1$ predicted at time k, respectively, and $A(\cdot)$ and $B(\cdot)$ are linear system approximations of the nonlinear dynamics at time k. By solving an optimal control problem over the prediction horizon, the optimal control input and the optimal mode sequence can be found. We then apply part of the optimal sequences $u(k|k), u(k+1|k), \ldots, u(k+N_u-1|K)$ and $\sigma(k+1|k), \sigma(k+2|k), \ldots, \sigma(k+N_u|k)$ over a control horizon N_u, and restart the whole process after N_u time. This process is repeated until the final time t_f is reached.

For the PHEV model, the MPC at each time step k solves the following constrained optimization problem:

$$\begin{aligned} \underset{u(t),\sigma(t)}{\text{minimize}} \quad & \sum_{i=0}^{N-1} J_i(x(k+i|k), u(k+i|k)) \\ \text{subject to} \quad & x(k+1+i|k) = A(i)x(k+i|k) + \\ & B(i)u(k+i|k) \\ & x^{min} \le x(k+i|k) < x^{max} \\ & u^{min} \le u(k+i|k) < u^{max} \end{aligned} \tag{23}$$

Note that the problem is subject to linear system dynamics and linear constraints on the state $x(k+i|k)$ and the input $x(k+i|k)$.

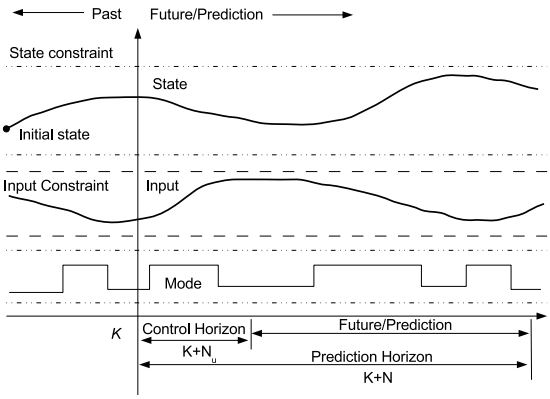

Fig. 10. Model predictive control.

1) Problem Formulation: We now formulate an energy optimizatoin problem for the power-split PHEV and present the hybrid model predictive control solution method. Solutions obtained by this method, though sub-optimal, can be implemented in real time.

The energy optimization problem is formulated as follows:

$$\begin{aligned} \underset{u(t),\sigma(t)}{\text{minimize}} \quad & \sum_{k=K}^{K+N-1} \frac{\omega_e(k)\tau_e(k)}{\eta(\omega_e(k), \tau_e(k))} + C_{eq}(\rho(k) - \rho(k+1)) \\ \text{subject to} \quad & x(k+1) = f(x(k), u(k)) \\ & \omega_e^{min} \le \omega_e(k+1) < \omega_e^{max} \\ & \upsilon^{min} \le \upsilon(k+1) < \upsilon^{max} \\ & \rho^{min} \le \rho(k+1) < \rho^{max} \\ & \omega_g^{min} \le (1+\varrho)/\varrho\omega_e - \omega_r/\varrho < \omega_g^{max} \\ & \tau_e^{min} \le \tau_e(k) < \tau_e^{max} \\ & \tau_g^{min} \le \tau_g(k) < \tau_g^{max} \\ & \tau_m^{min} \le \tau_m(k) < \tau_m^{max} \end{aligned} \tag{24}$$

In the above problem, the objective is to minimize the energy consumption of the PHEV. The first part of the objective function is the energy used by the engine, which can be expressed as a ratio of the output mechanical power ω_e over the engine efficiency η. The second part of the objective function is the energy used by the battery, which is given by the difference in the state of charge ρ of the battery, multiplied

by a certain constant C_{eq}. There are constraints on the state and the input in (24) as well.

Note that in (24) the engine power term is a nonlinear term. To solve this problem efficiently, the engine power term has been approximated by a quadratic function of the engine speed ω_e and the engine torque ω_e. Furthermore, the dynamics of the PHEV in EV, Regen, Hybrid and Batterycharge modes as given by (16) [16] are nonlinear dynamics. These dynamics are repeatedly linearized at constant time intervals to yield piece-wise linear dynamics approximations given by the matrices $A(\cdot)$ and $B(\cdot)$:

$$x(k+i+1|k) = A(k)x(k+i|k) + B(k)u(k+i|k), \quad (25)$$

where

$$A(k) = \frac{\partial f}{\partial x}(x_e, u_e) = \begin{bmatrix} \frac{\partial f_1}{\partial x_1} & \cdots & \frac{\partial f_1}{\partial x_n} \\ \vdots & \ddots & \vdots \\ \frac{\partial f_n}{\partial x_1} & \cdots & \frac{\partial f_1}{\partial x_n} \end{bmatrix} \quad (26)$$

$$B(k) = \frac{\partial f}{\partial u}(x_e, u_e) = \begin{bmatrix} \frac{\partial f_1}{\partial u_1} & \cdots & \frac{\partial f_1}{\partial u_n} \\ \vdots & \ddots & \vdots \\ \frac{\partial f_n}{\partial u_1} & \cdots & \frac{\partial f_1}{\partial u_n} \end{bmatrix}. \quad (27)$$

After the above approximation, the objection function is quadratic and all the constraints are linear. Thus, the optimization problem can be re-formulated as a linearly constrained, quadratic optimization problem as follows:

$$\begin{aligned} \underset{u(t),\sigma(t)}{\text{minimize}} \quad & U^T H U + U^T F \\ \text{subject to} \quad & GU \leq W \\ & U^{min} \leq U \leq U^{max} \end{aligned} \quad (28)$$

In this equation, the control sequence over the prediction horizon $u(K)\ u(K+1)\ u(k+1), \ldots, u(k+N-1)$ have been vectorized by the vector U. During the entire prediction horizon the vehicle model is assumed to be represented by the linear model (25). The optimal mode sequence $\sigma(k+1|k), \sigma(k+2|k) \cdots \sigma(k+N_u|k)$ is obtained based on the power input P_e by the engine and the state of charge ρ of the battery.

IV. Simulation Results

Comment: in this section (including subsections A,B,C below) more detailed discussions on the implications of the simulation results are welcome. The PHEV considered in the simulation has a 57 kWh engine, a 50 kWh MG1 motor, and a 5 kWh battery pack. More details on the vehicle specifications are given in Table I. Vehicle is simulated for an EPA Urban Dynamometer Drive Schedule (UDDS). Total distance travelled by the vehicle for this drive cycle is 7.3 miles in 1370 seconds. Details on EPA and Highway (HWFET) drive cycle are provided in Table II. Matlab/Simulink environment is used to to simulate the hybrid dynamical system model of PHEV.

The primary benefit of the PHEVs comes from maximizing the use of electrical energy while it is available. Starting from 95% until 30% SOC, maximum electrical energy should be used by driving the vehicle in only two modes, EV mode or Regen mode. From 30% to 25% SOC vehicle can operate in EV mode, Regen mode, Hybrid mode or BatteryChg mode depending on the driver demands.

TABLE I
Vehicle Specifications

Component	Specifications
Engine	57 kW
Motor (MG1)	50 kW PM motor
Generator (MG2)	30 kW PM motor
Battery chemistry	Li-Ion
Battery capacity	6.3 kWh
Transmission	Planetary Gear set (CVT)

TABLE II
Drive cycle characteristics

Characteristic	City Drive	Highway Drive
Distance(miles)	7.45	10.2
Time(s)	1369	765
Max speed(Mph)	56.7	60
Average speed(Mph)	19.58	48.3
Max acceleration($\frac{m}{s^2}$)	1.47	1.43
Max deceleration($\frac{m}{s^2}$)	-1.47	1.47
Average acceleration($\frac{m}{s^2}$)	0.50	0.19
Average deceleration($\frac{m}{s^2}$)	-0.58	0.22
Idle time(s)	259	6
Number of stops	17	1

To simulate the PHEV driving in city conditions with almost fully charged battery (95% SOC), the vehicle is simulated for 4 consecutive drive cycles as shown in Figure 11 with a total travel distance of 29 miles in 1.5 hours. The simulation results for the dynamic programming and model predictive hybrid control (MPHC) are presented in Section IV-A and Section IV-B, respectively.

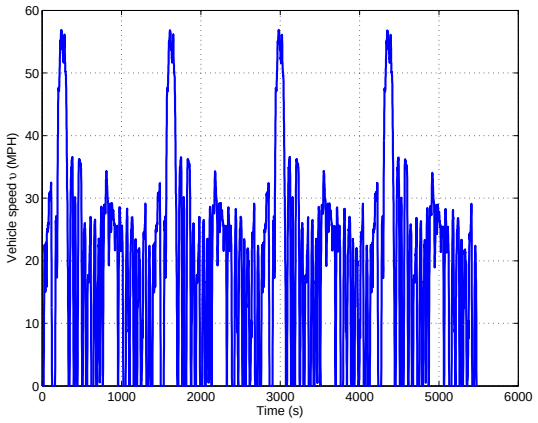

Fig. 11. Four consecutive urban dynamometer drive schedules by the EPA.

A. Results of Dynamic Programming Method

The PHEV vehicle is simulated for four UDDS drive cycles. Once the SOC of the battery reaches 30%, the dynamic programming method is applied to select the operational mode

σ and the input u to the system. Fig. 13 shows the vehicle speed v while following the UDDS drive cycles under the dynamic programming controller.

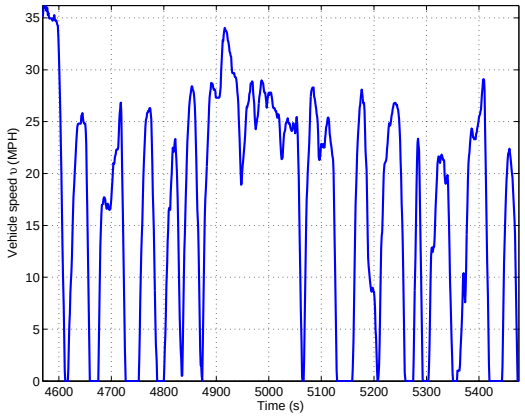

Fig. 12. Vehicle speed while following the UDDS drive cycles using dynamic programming.

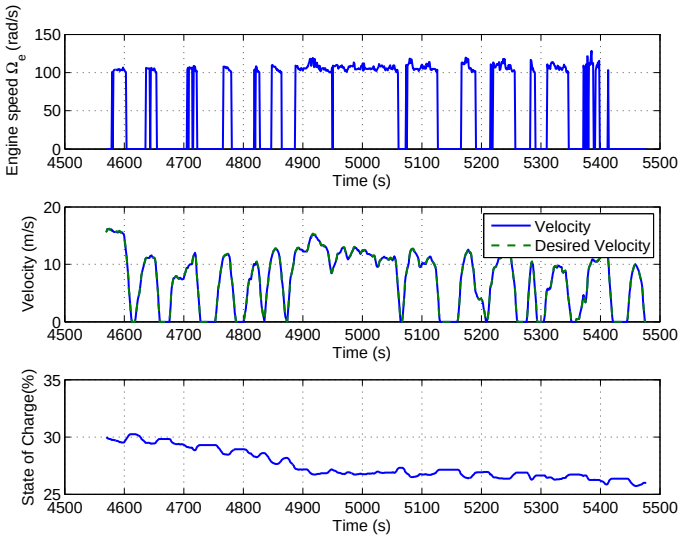

Fig. 13. Vehicle speed while following the UDDS drive cycles using dynamic programming.

Fig. 13 shows the state of charge ρ of the battery, which is charged in the Regen mode and the Battery charge mode; and discharged in the EV mode and the Hybrid Mode. The SOC starts from 30% and depletes until 26%. Thus, the energy from the battery is blended with the energy from the engine to drive the vehicle. Additionally, it shows the Engine speed, which is operated around low ideal speed most of the time while vehicle is satisfying desired performance of desired speed.

Figure 14 shows the input torques for engine, generator and m otor. It shows that Engine torque increases as the State of charge of battery lowers, to produce extra power to charge battery. Meanwhile, generator provides reactionary torque and motor recuperates vehicle energy while braking.

In Fig. 15 the operational mode σ under the dynamic programming controller is shown. In this figure, the mode

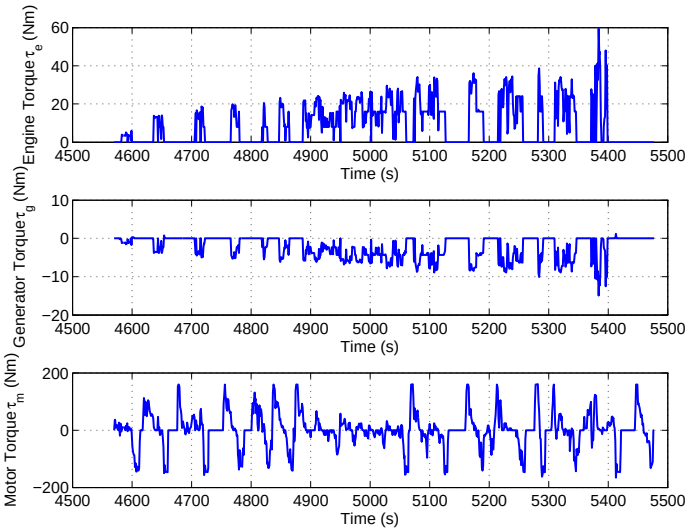

Fig. 14. Vehicle speed while following the UDDS drive cycles using dynamic programming.

values of 0,1,2,3,4 correspond to the stationary mode, the EV mode, the Regen mode, the Hybrid mode, and the Battery charge mode, respectively.

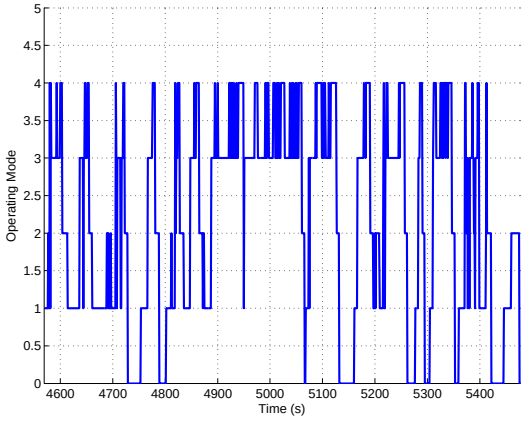

Fig. 15. Optimal mode selection in Dynamic programming for UDDS drive cycle.

B. Model Predictive Hybrid control results

In model predictive hybrid control, when the SOC falls below 30% the modes of operation of the PHEV will be more. Once the SOC reaches 30% the model predictive hybrid controller is applied to determine the operation mode. The prediction horizon is set to be 5 seconds, while the control horizon is 1 second. Similar to dynamic programming, Fig. 16 shows the vehicle speed v while following part of UDDS drive cycles under the model predictive hybrid controller.

Fig. 16 shows the SOC of the PHEV battery while the vehicle is under the model predictive hybrid controller. The SOC starts from 30% and depletes until reaching 26%. The vehicle operates in the EV mode, the Regen mode, the Hybrid mode and the Battery charge mode which is very similar to

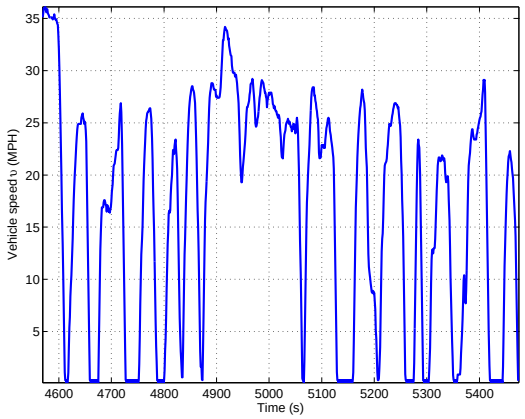

Fig. 16. PHEV speed while following UDDS drive cycle for Model Predictive hybrid control.

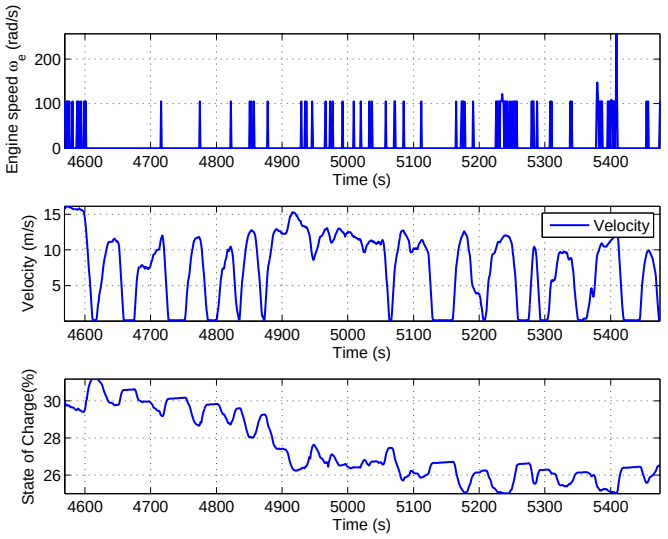

Fig. 17. Vehicle speed while following the UDDS drive cycles using dynamic programming.

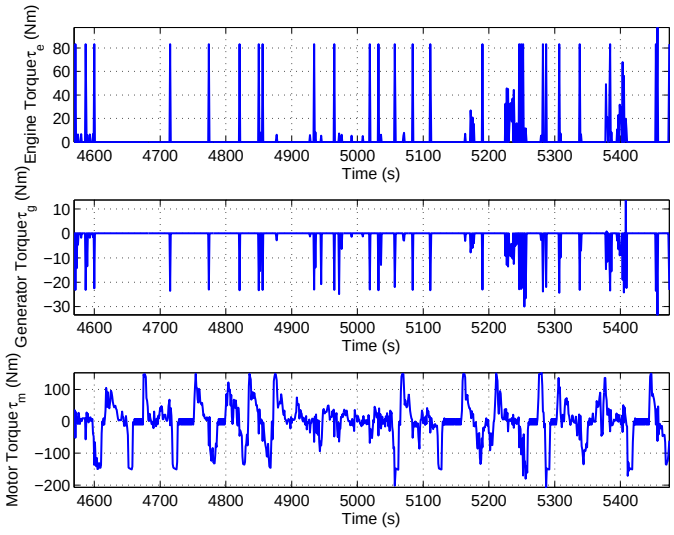

Fig. 18. Vehicle speed while following the UDDS drive cycles using dynamic programming.

the case when using the dynamic programming controller. Additionally, engine is operated at lower speed most of the time close to idle speed while satisfying desired vehicle speed performance.

Fig. 18 shows input commands of engine generator and motor. In this strategy, the Engine is operated mostly at higher torques as state of charge is close to its lower limit. Meanwhile, generator provides reactionary torque to engine and motor recovers energy from the vehicle by regenerative braking.

Fig. 19 shows the the operational mode σ when the vehicle is under the model predictive hybrid control. Similar to Fig. 15, the mode values of 1,2,3,4 correspond to the EV mode, the Regen mode, the Hybrid mode, and the Battery charge mode, respectively.

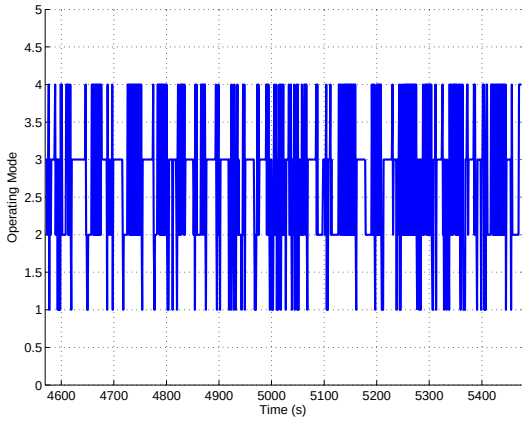

Fig. 19. Operational mode of PHEV for Model Predictive hybrid control.

This Model Predictive Hybrid control based EMS has been evaluated in real time using dSPACE controller. Both Vehicle model and Energy Management System has been implemented in Real-time using Dspace controller.

C. Comparing Dynamic programming and Model Predictive Hybrid control

When the optimization problem is solved by dynamic programming, it calculates the optimum input sequence and the optimum mode sequence based on the current cost and future cost-to-go. Whereas model predictive hybrid control solves an optimization problem and obtained the optimum inputs and optimum mode selection based on the current cost and future cost-to-go calculated over the prediction horizon. Hence, model predictive hybrid control would provide sub-optimal results as compared to the dynamic programming method. In this study, as shown in Fig. 20, the energy cost of driving the vehicle over the same EPA city drive cycle (UDDS) for the model predictive hybrid control is 4.25% larger than the dynamic programming results. In addition, these two controllers were compared through simulations using the EPA Highway drive cycle (HWFET). The results showed that the model predictive hybrid control is 4.85% suboptimal compared to the dynamic programming results. Considering that the

model predictive hybrid controller can be implemented on the vehicle in real time, this sub-optimality is acceptable.

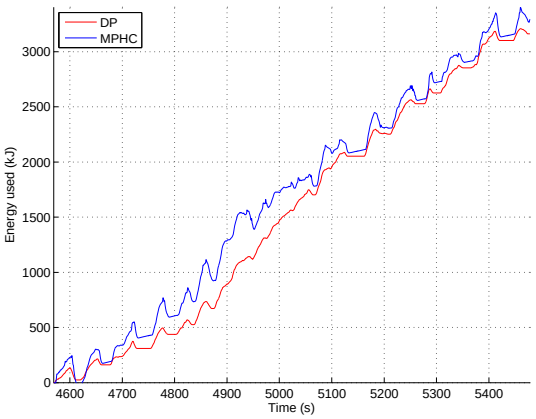

Fig. 20. Energy used by vehicle following UDDS drive cycle for Model predictive hybrid control.

V. Conclusion

This paper demonstrates a novel approach to modeling the power-split plug-in hybrid electric vehicle using the hybrid dynamical system theory. To design a supervisory energy management strategy for the PHEV, an energy optimization problem is solved using the dynamic programming approach for hybrid dynamical systems. The results obtained from this approach are optimal but can incur large computational time. For real-time implemention, a sub-optimal model predictive hybrid controller is designed. Results show that the model predictive hybrid control can be implemented in real-time and can provide a very good approximation of the global optimal solution obtained by the dynamic programming approach. Furthermore, the hybrid dynamical system modeling and the supervisory energy management system design approach can be extended to hybrid electric vehicles of power-split drivetrain or any other drivetrain.

References

[1] S. P. D. Karbowski, A. Rousseau and P. Sharer, "Plug-in vehicle control strategy: from global optimization to rea-time application," in *Electric Vehicle Symposium (EVS23), Anaheim, California*, Dec 2007.

[2] B. Baumann, G. Washington, B. Glenn, and G. Rizzoni, "Mechatronic design and control of hybrid electric vehicles," *Mechatronics, IEEE/ASME Transactions on*, vol. 5, no. 1, pp. 58 –72, mar 2000.

[3] H. Banvait, S. Anwar, and Y. Chen, "A rule-based energy management strategy for plug-in hybrid electric vehicle (phev)," in *American Control Conference, 2009. ACC '09.*, june 2009, pp. 3938 –3943.

[4] L. Sun, R. Liang, and Q. Wang, "The control strategy and system preferences of plug-in hev," in *Vehicle Power and Propulsion Conference, 2008. VPPC '08. IEEE*, sept. 2008, pp. 1 –5.

[5] P. Sharer, A. Rousseau, D. Karbowski, and S. Pagerit, "Plug-in hybrid electric vehicle control strategy: Comparison between ev and charge-depleting options," *SAE paper*, pp. 01–0460, 2008.

[6] Y. Gao and M. Ehsani, "Design and control methodology of plug-in hybrid electric vehicles," in *Vehicle Power and Propulsion Conference, 2008. VPPC '08. IEEE*, sept. 2008, pp. 1 –6.

[7] A. Rousseau, S. Pagerit, and D. Gao, "Plug-in hybrid electric vehicle control strategy parameter optimization," *Journal of Asian Electric Vehicles*, vol. 6, no. 2, pp. 1125–1133, 2008.

[8] X. Wu, B. Cao, J. Wen, and Y. Bian, "Particle swarm optimization for plug-in hybrid electric vehicle control strategy parameter," in *Vehicle Power and Propulsion Conference, 2008. VPPC '08. IEEE*, sept. 2008, pp. 1 –5.

[9] S. P. Q. Cao and A. Rousseau, "Phev hymotion prius model validtion and control improvements," in *Electric Vehicle Symposium (EVS23), Anaheim, California*, Dec 2007.

[10] F. Syed, M. Kuang, J. Czubay, and H. Ying, "Derivation and experimental validation of a power-split hybrid electric vehicle model," *Vehicular Technology, IEEE Transactions on*, vol. 55, no. 6, pp. 1731 –1747, nov. 2006.

[11] Q. Gong, Y. Li, and Z. Peng, "Power management of plug-in hybrid electric vehicles using neural network based trip modeling," in *American Control Conference, 2009. ACC '09.*, june 2009, pp. 4601 –4606.

[12] S. Moura, D. Callaway, H. Fathy, and J. Stein, "Impact of battery sizing on stochastic optimal power management in plug-in hybrid electric vehicles," in *Vehicular Electronics and Safety, 2008. ICVES 2008. IEEE International Conference on*, sept. 2008, pp. 96 –102.

[13] Y. Bin, Y. Li, Q. Gong, and Z.-R. Peng, "Multi-information integrated trip specific optimal power management for plug-in hybrid electric vehicles," in *American Control Conference, 2009. ACC '09.*, june 2009, pp. 4607 –4612.

[14] J. Liu and H. Peng, "Modeling and control of a power-split hybrid vehicle," *Control Systems Technology, IEEE Transactions on*, vol. 16, no. 6, pp. 1242 –1251, nov. 2008.

[15] S. Stockar, V. Marano, M. Canova, G. Rizzoni, and L. Guzzella, "Energy-optimal control of plug-in hybrid electric vehicles for real-world driving cycles," *Vehicular Technology, IEEE Transactions on*, vol. 60, no. 7, pp. 2949 –2962, sept. 2011.

[16] H. Borhan, A. Vahidi, A. Phillips, M. Kuang, I. Kolmanovsky, and S. Di Cairano, "Mpc-based energy management of a power-split hybrid electric vehicle," *Control Systems Technology, IEEE Transactions on*, vol. 20, no. 3, pp. 593 –603, may 2012.

[17] C. Musardo, G. Rizzoni, and B. Staccia, "A-ecms: An adaptive algorithm for hybrid electric vehicle energy management," in *Decision and Control, 2005 and 2005 European Control Conference. CDC-ECC '05. 44th IEEE Conference on*, dec. 2005, pp. 1816 – 1823.

[18] H. Banvait, X. Lin, S. Anwar, and Y. Chen, "Plug-in hybrid electric vehicle energy management system using particle swarm optimization," *World Electric Vehicle Journal*, vol. 3, no. 1, 2009.

[19] X. Lin, H. Banvait, S. Anwar, and Y. Chen, "Optimal energy management for a plug-in hybrid electric vehicle: Real-time controller," in *American Control Conference (ACC), 2010*, 30 2010-july 2 2010, pp. 5037 –5042.

[20] M. F. ZMorteza Mohebbi, "Adaptive neuro control of parallel hybrid electric vehicles," *International Journal of Alternative propulsion*, vol. 1, no. 1, pp. 3–19, 2007.

[21] R. G. Baumann, B. and G. Washington, "Intelligent control of hybrid vehicles using neural networks and fuzzy logic," *SAE paper*, pp. 02–23, 1998.

[22] J. Moreno, M. Ortuzar, and J. Dixon, "Energy-management system for a hybrid electric vehicle, using ultracapacitors and neural networks," *Industrial Electronics, IEEE Transactions on*, vol. 53, no. 2, pp. 614 – 623, april 2006.

[23] Q. Gong, Y. Li, and Z.-R. Peng, "Optimal power management of plug-in hev with intelligent transportation system," in *Advanced intelligent mechatronics, 2007 IEEE/ASME international conference on*, sept. 2007, pp. 1 –6.

[24] Y. Zhu, Y. Chen, Z. Wu, and A. Wang, "Optimisation design of an energy management strategy for hybrid vehicles," *International Journal of Alternative propulsion*, vol. 1, no. 1, p. 47, 2006.

PLACE PHOTO HERE

Harpreetsingh Banvait Harpreetsingh Banvait received his M.S. degree in Electrical and Computer Engineering from Indiana University-Purdue University Indianapolis (IUPUI), Indianapolis, Indiana. Currently, he is pursuing his Ph.D. degree in Electrical and Computer Engineering at Purdue University, West Lafayette, Indiana. His research interests are in intelligent control, optimal control, discrete control, hybrid systems control, and automotive control systems.

PLACE PHOTO HERE

Jianghai Hu received the B.E. degree in automatic control from Xian Jiaotong University, P.R. China, in 1994, and the M.A. degree in Mathematics and the Ph.D. degree in Electrical Engineering from the University of California, Berkeley, in 2002 and 2003, respectively. He is currently an assistant professor at the School of Electrical and Computer Engineering, Purdue University. His research interests include hybrid systems, multiagent coordinated control, control of systems with uncertainty, and applied mathematics.

PLACE PHOTO HERE

Yaobin Chen Yaobin Chen received his Ph.D. degree in Electrical Engineering from Rensselaer Polytechnic Institute, Troy, New York, in 1988. Dr. Chen is a senior member of IEEE, a member of SAE and ASEE. He is currently Professor and Chair of Electrical and Computer Engineering, and Director of the Transportation Active Safety Institute in the Purdue School of Engineering and Technology, Indiana University-Purdue University Indianapolis (IUPUI). Dr. Chen's current research interests are modeling, control, optimization, and simulation of advanced transportation and automotive systems, energy and power systems, computational intelligence and its applications.